

---

# Disentangling Voice and Content with Self-Supervision for Speaker Recognition

---

Tianchi Liu<sup>1, 2</sup>, Kong Aik Lee<sup>\*3, 1</sup>, Qionqiong Wang<sup>1</sup>, Haizhou Li<sup>4, 2</sup>

<sup>1</sup> Institute for Infocomm Research (I<sup>2</sup>R), Agency for Science, Technology and Research (A\*STAR), Singapore

<sup>2</sup> Dept. of Electrical and Computer Engineering, National University of Singapore, Singapore

<sup>3</sup> Dept. of Electrical and Electronic Engineering, Hong Kong Polytechnic University, Hong Kong

<sup>4</sup> School of Data Science, The Chinese University of Hong Kong, Shenzhen, China

{liu\_tianchi, wang\_qionqiong}@i2r.a-star.edu.sg, kongaik.lee@ieee.org, haizhouli@cuhk.edu.cn

## Abstract

For speaker recognition, it is difficult to extract an accurate speaker representation from speech because of its mixture of speaker traits and content. This paper proposes a disentanglement framework that simultaneously models speaker traits and content variability in speech. It is realized with the use of three Gaussian inference layers, each consisting of a learnable transition model that extracts distinct speech components. Notably, a strengthened transition model is specifically designed to model complex speech dynamics. We also propose a self-supervision method to dynamically disentangle content without the use of labels other than speaker identities. The efficacy of the proposed framework is validated via experiments conducted on the VoxCeleb and SITW datasets with 9.56% and 8.24% average reductions in EER and minDCF, respectively. Since neither additional model training nor data is specifically needed, it is easily applicable in practical use.

## 1 Introduction

Automatic speaker recognition aims to identify a person from his/her voice [2] based on speech recordings [24]. Typically, two fixed-dimensional representations are extracted from the enrollment and test speech utterances, respectively [77]. Then the recognition procedure is done by measuring their similarity [24]. These representations are referred to as the speaker embeddings [76]. The concept of speaker embedding is similar to that of the face embedding [72] in the face recognition task and the token embedding [18] in the language model, while the main difference lies in the carriers of the information source and the nature of downstream tasks. Different from the discrete sequential inputs in Natural Language Processing (NLP) and continuous inputs in Computer Vision (CV), speech signals are continuous-valued variable-length sequences [26]. Speech signals contain both speaker traits and content [38]. For speaker recognition, to form a refined speaker embedding of a speech signal, conventional methods aggregate the frame-level features by pooling across the time-axis to extract speaker characteristics while factoring out content information. Simple temporal aggregation fails to disentangle the content information and therefore affects the quality of the resulting embeddings. The content information is regarded as unwanted variations hindering the accurate representation of voice characteristics.

To reduce the effects of the content variation, prior works model the phonetic content representation and use it as a reference for speaker embedding extraction. In [101], the phonetic bottleneck features from the last hidden layer of a pre-trained automatic speech recognition (ASR) network are combined with raw acoustic features to normalize the phonetic variations. A coupled stem is designed in [100] to jointly learn acoustic features and frame-level ASR bottleneck features. In [49], a phonetic attention mask dynamically generated from a sub-branch is used to benefit speaker recognition. The existing methods can be summarized into two types in terms of content representation modeling: (1) by a

---

\*Corresponding author.

pre-trained ASR model [64, 41, 52, 101, 53], and (2) by a jointly trained multi-task model with extra components for content representations [50, 100, 19, 53, 91, 51, 49]. These methods prove that the utilization of content representation benefits speaker recognition. However, both types lead to an obvious limit in practical applications. The employment of a pre-trained ASR model greatly increases the parameters and computation complexity in the inference, as the ASR models are typically one or two orders of magnitude larger than the speaker recognition model [99, 80]. The joint training of the speaker recognition model and extra components for content representations requires either an extra dataset with text labels in addition to the dataset with speaker identities, or one dataset with speaker identities and text labels simultaneously which is expensive and not easy to come by. For the former type of joint training, additional components are still needed with extra effort and may encounter optimization difficulties.

For the purpose of speaker recognition, one aims to derive an embedding vector representing the vocal characteristics of the speaker. The benefits of leveraging content representation are significant, while the drawbacks of text labels and extra model requirements are obvious. Motivated by this, we seek to design a novel framework to solve these problems.

Speech signals consist of many components, of which the two major parts are speaker traits and speech content [38, 15]. In this paper, we focus on decomposing speech signals into static and dynamic components. The former is static, i.e., fixed, with respect to temporal evolution and dominated by speaker characteristics, while the latter mainly consists of speech content with some other components, such as the prosody. Based on this assumption, we design a framework with three Gaussian inference layers which aims to decompose the static and dynamic components of the speech. The static part is modeled by static Gaussian inference with the criterion of speaker classification loss. During inference, the static latent factor is associated with the vocal characteristics of the speaker, and we refer to it as speaker representation. The remaining dynamic components related to verbal content are modeled by dynamic Gaussian inference. The motivation of the three-layer design is simple and intuitive – the speaker representation from *layer 1* is not accurate and may include content information as the content-related reference is absent in training. However, it helps *layer 2* extract the content representation which can be used as the reference for *layer 3*. Thus, a more accurate speaker representation is extracted in *layer 3*. It is worth noting that the framework is trained without text labels and no extra model or branch is employed thus not much increase in model size. This is achieved with the guide of self-supervision and considered content representations. We named this framework as **Recurrent Xi-vector (RecXi)**. The major contributions are summarized as follows:

- **RecXi: A novel disentangling framework** with the following features: (1) We enhance the xi-vector [39] with the ability to capture temporal information and name it the recurrent xi-vector layer. (2) A frame-wise content-aware transition model  $\mathbf{G}_t$  is proposed for modeling dynamic components of the speech. (3) A novel design of three layers of Gaussian inference is proposed to disentangle speaker and content representations by static and dynamic modeling with the corresponding counterpart removal, respectively.
- **A self-supervision method** is proposed to guide content disentanglement by preserving speaker traits. It reduces the impact of the absence of text labels.

## 2 Related Work

**Conventional Speaker Recognition Methods.** Speaker embeddings are fixed-length continuous-value vectors extracted from variable-length utterances to represent speaker characteristics. They live in a simpler Euclidean space in which distance can be measured for the comparison between speakers [89]. A well-known example of the extractor is the x-vector framework [76], which mainly consisted of the following three components: **1). An encoder** is implemented by stacking multiple layers of time-delay neural network (TDNN) and used to extract the frame-level features from utterances [66]. Recent works strengthen the encoder by replacing the simple TDNNs with powerful ECAPA-TDNN [17] and its variants [48, 83, 25, 60, 54], or ResNet series models [102, 43, 96, 95, 58]. **2). A temporal aggregation layer** aggregates frame-level features from the encoder into fixed-length utterance-level representations. **3). A decoder** classifies the utterance-level representations to speaker classes for supervised learning by a classification loss. The decoder stacks several fully-connected layers including one bottleneck layer used to extract speaker embedding.

**Speech Disentanglement.** Various informational factors are carried by the speech signal, and the speech disentanglement ultimately depends on which informational factors are desired and how they

will be used [92]. For speaker recognition, in addition to the use of content information we introduced above, some works attempt to disentangle speaker representation with the removal of irrelevant information, like devices, noise, and channel information with corresponding labels [57, 59, 30]. [59] minimizes the mutual information between speaker and device embeddings, with the goal of reducing their interdependence. In [47], nuisance variables like gender and accent are removed from speaker embeddings by learning two separate orthogonal representations. Many other speech-relevant tasks also show great improvements by disentangling these two components properly. For speaker diarization, the ASR model is employed to obtain content representations leveraged by speaker embedding extractions [79, 32]. In voice conversion or personalized voice generation tasks, a popular method is to disentangle the speech into linguistic and speaker representations before performing the generation [28, 98, 104, 12, 20, 103, 45]. In ASR, speaker information is extracted for speaker variants removal for performance improvements [56, 42, 27] or privacy preserving [78]. Similarly, auxiliary network-based speaker adaptation [71] or residual adapter [85] are explored to handle large variations in the speech signals produced by different individuals. These works have led us to the design of RecXi, which is the first speaker and content disentanglement framework for speaker recognition in the absence of extra labels for practical use to the best of our knowledge.

**Self-Supervision in Speech.** Self-supervised learning has been the dominant approach for utilizing unlabeled data with impressive success [1, 18, 8, 22]. In speaker recognition, *contrastive learning* [10] is used to force the encoder to produce similar activation between a positive pair. The positive pair can be two disjoint segments from the same utterance [6, 97] or from cross-referencing between speech and face data [82]. The trained speaker encoder also can produce pseudo speaker labels for supervised learning [81, 5]. In target speaker extraction, self-supervision is helpful to find the speech-lip synchronization [63]. In voice conversion, much research focuses on applying *variational auto-encoder* (VAE) to disentangle the speaker [11, 29, 67]. Similar to reconstruction-based methods, mutual information (MI) and identity change loss are used in [36] for robust speaker disentanglement. ContentVec [68] disentangles and removes speaker variations from the speech representation model HuBERT [26] for various downstream tasks, such as language modeling and zero-shot content probe.

Considering the main objective of this work is to benefit speaker recognition by disentangling the speaker with the speaker classification supervision, we want to clarify that the content disentanglement and corresponding self-supervision serve this final target. Therefore, the self-supervision method is designed to be simple yet effective while avoiding extra signal re-constructors or training efforts.

### 3 Approach

#### 3.1 Xi-vector

Many works have been proposed to estimate the uncertainty for the speaker embedding [73, 39, 89]. Among them, the xi-vector [39] is proposed to enhance x-vector embedding in handling the uncertainty caused by the random intrinsic and extrinsic variations of human voices. Specifically, an input frame  $\mathbf{x}_t$  is encoded to a point-wise estimate  $\mathbf{z}_t$  in a latent space by an encoder. And an auxiliary network is employed to characterize the frame-level uncertainty with a posterior covariance matrix  $\mathbf{L}_t^{-1}$  associated with  $\mathbf{z}_t$  as shown in the encoder part of Figure 1. These two operations are formulated as

$$\mathbf{z}_t = f_{\text{enc}}(\mathbf{x}_t | \mathbf{x}_t^{t \pm n}), \quad (1) \quad \log \mathbf{L}_t = g_{\text{enc}}(\mathbf{x}_t | \mathbf{x}_t^{t \pm n}), \quad (2)$$

where the neighbour frames  $\mathbf{x}_t^{t \pm n}$  of time  $t$  are taken into consideration for the frame-wise estimation. The precision matrices  $\mathbf{L}_t$  are assumed to be diagonal and are estimated as log-precision for the convenience of following steps. It is assumed that a *linear Gaussian model* is responsible to generate the representations  $\mathbf{z}_t$  as follows:

$$\text{generative model : } \mathbf{z}_t = \mathbf{h} + \epsilon_t, \text{ latent variable : } \mathbf{h} \sim \mathcal{N}(\phi_p, \mathbf{P}_p^{-1}), \text{ uncertainty : } \epsilon_t \sim \mathcal{N}(\mathbf{0}, \mathbf{L}_t^{-1}). \quad (3)$$

Here,  $\mathbf{h}$  is the latent variable for the entire utterance, and  $\epsilon_t$  is a frame-wise random variable for the uncertainty covariance measure,  $\phi_p$  and  $\mathbf{P}_p^{-1}$  are the Gaussian prior mean and covariance matrix of the variable  $\mathbf{h}$ . The posterior mean vector  $\phi_s$  and precision matrix  $\mathbf{P}_s$  for the whole sequence are formulated as

$$\phi_s = \mathbf{P}_s^{-1} \left[ \sum_{t=1}^T \mathbf{L}_t \mathbf{z}_t + \mathbf{P}_p \phi_p \right], \quad (4) \quad \mathbf{P}_s = \sum_{t=1}^T \mathbf{L}_t + \mathbf{P}_p, \quad (5)$$

where the posterior mean  $\phi_s$  is enriched by frame-wise uncertainty and is further used to be decoded into speaker embedding.

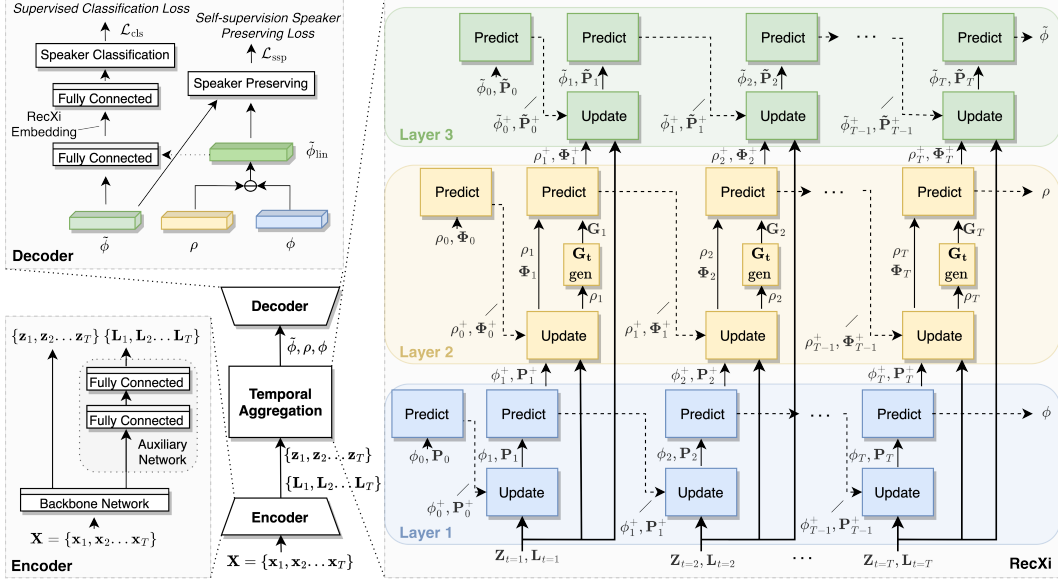


Figure 1: The network architecture of the proposed RecXi system with self-supervision. The structure at the bottom-middle of the figure is a simplified speaker recognition system. The figures in three dotted boxes are the specific explanations of its three parts. At the encoder,  $\{x_1, x_2 \dots x_T\}$  is the input sequence of length  $T$ . The three colors of blue, orange, and green indicate three recursive layers. For each layer, the inference flow for frames  $x_1, x_2$  and  $x_T$  is drawn, while the frames in between are replaced by ‘...’. The dashed lines indicate recurrent operation and the solid lines represent the operations within the same frame. The block with  $G_t$  gen indicates the filter generator. For the decoder,  $\ominus$  is a subtraction operation. The dotted line indicates the operation is optional.

### 3.2 Disentangling Speaker and Content Representations

**Basic Recurrent Xi-vector Layer.** Xi-vector has the advantage of modeling static components of the speech by the utterance-level speaker representation aggregation with the use of uncertainty estimation, while the drawback of modeling dynamic signals is obvious. For approximating non-linear functions in high-dimensional feature spaces and restricting the inference through the adjacent Gaussian hidden state efficiently, similar to [4], a learnable linear transition model  $\mathbf{G}$  is applied. We further extend the xi-vector into a recursive form with frame-level estimation. It is worth noting that xi-vector is a special case of the basic recurrent xi-vector when  $\mathbf{G}$  is an identity matrix.

The Gaussian inference in the latent space can be implemented in two stages: *predict stage* and *update stage*. In the *predict stage*, the predictive mean vector  $\rho_t^+$  and precision matrix  $\Phi_t^+$  are formulated as

$$\rho_t^+ = \mathbf{G}\rho_t, \quad (6) \quad \Phi_t^+ = [\mathbf{G}\Phi_t^{-1}\mathbf{G}^T]^{-1}, \quad (7)$$

where  $\mathbf{G}$  represents a linear transition model, and  $^+$  indicates the results of the given frame  $t$  after the *predict stage*.  $\mathbf{T}$  indicates a transpose operation.

For sake of clarity, we assign the time (i.e., frame) index  $t = 0$  to the priors, such that  $\rho_0 = \rho_p, \Phi_0 = \Phi_p$ . In the *update stage*, the posterior mean vector  $\rho_t$  of frame  $t$  is derived by incorporating the previously predicted posterior mean and precision  $\{\rho_{t-1}^+, \Phi_{t-1}^+\}$  of the hidden states of the former frame  $t - 1$  with encoded features  $\mathbf{z}_t$  and estimated uncertainty  $\mathbf{L}_t$  of current frame  $t$ . The uncertainty measures  $\mathbf{L}_t$  of frame  $t$  is added into the posterior precision matrix. These two operations are derived as

$$\rho_t = \Phi_t^{-1}[\mathbf{L}_t\mathbf{z}_t + \Phi_{t-1}^+\rho_{t-1}^+], \quad (8) \quad \Phi_t = \mathbf{L}_t + \Phi_{t-1}^+. \quad (9)$$

**Frame-wise Content-aware Transition Model  $\mathbf{G}_t$ .** Speech signals are a complex mixture of dynamic information sources. Even though the transition model  $\mathbf{G}$  is learnable during training, it remains the same across all the hidden states of Gaussian inference for each sample. To enhance the ability to model dynamic speech components for content disentanglement, we propose a transition

model  $\mathbf{G}_t$  which is dynamically adjusted by a filter generator for each frame according to the content during the Gaussian inference and hereby named frame-wise content-aware transition model.

Specifically, a set of  $N$  learnable transition matrices  $\{\mathbf{G}'_1, \mathbf{G}'_2 \dots \mathbf{G}'_N\}$  is employed to model  $N$  dynamic components in speech signals. For each frame  $t$ , a vector  $\mathbf{w}_t \in \mathbb{R}^N$  is generated representing the importance of different dynamic components to content representation modeling, by observing content information  $\rho_t$  from *update stage*. The content-aware transition model for frame  $t$  is finally obtained as a weighted sum over the  $N$  component-dependent transition models with weight  $w_{t,n}$ .

$$\mathbf{G}_t = \sum_{n=1}^N w_{t,n} \mathbf{G}'_n, \quad (10) \quad w_{t,n} = [\mathbf{w}_t]_n, \quad (11) \quad \mathbf{w}_t = \sigma(f(\rho_t)), \quad (12)$$

where  $\mathbf{w}_t \in \mathbb{R}^N$ .  $\sigma$  and  $f$  indicate the *Softmax* function and a non-linear operation, respectively. In this work, the non-linear operation is designed as two fully connected layers with a ReLU [21] activation function in between. It is to be noted that this procedure is frame-wise as the dynamic components vary along the sequence of  $T$ . As an extension to Equations (6) and (7), the *predict stage* of recurrent xi-vector is reformulated as

$$\rho_t^+ = \mathbf{G}_t \rho_t, \quad (13) \quad \Phi_t^+ = [\mathbf{G}_t \Phi_t^{-1} \mathbf{G}_t^T]^{-1}. \quad (14)$$

**Three Layers of Gaussian Inference.** We propose a structure based on three layers of Gaussian inference for disentangling speaker and content representations in the absence of text labels. In this work, this structure is utilized in the temporal aggregation layer and named RecXi. The three layers of Gaussian inferences each aim at precursor speaker representation, disentangled content representation, and disentangled speaker representation, as shown in the RecXi part of Figure 1. The last frame’s representations from each layer are used for deriving embeddings within the decoder. The details of each layer are discussed as follows.

**Layer 1: Precursor Speaker Representation.** This is a basic recurrent xi-vector layer that aims to represent the speaker characteristics. Therefore, the transition model of the Gaussian inference is set as an identity matrix to model static components of the speech. The *predict stage* can be derived from Equations (6) and (7) as

$$\phi_t^+ = \phi_t, \quad (15) \quad \mathbf{P}_t^+ = \mathbf{P}_t. \quad (16)$$

The speaker representation from this layer is similar to that in the original xi-vector, where the content information from the high-dimensional frame-level features remains and affects the speaker embedding quality. We refer to the representation of this layer as the precursor speaker representation. Specifically, the frame-wise representations of posterior mean  $\phi_t$  and precision  $\mathbf{P}_t$  of the hidden state  $\mathbf{h}$  of frame  $t$  are estimated. They are derived partly according to frame-level features  $\mathbf{z}_t$  and uncertainty  $\mathbf{L}_t$  extracted from the corresponding frame  $t$ , and partly from previous frames  $\{1, 2, \dots, t-1\}$  by recursively passing in the posteriors from the previous frame. The *update stage* is formulated as

$$\phi_t = \mathbf{P}_t^{-1} [\mathbf{L}_t \mathbf{z}_t + \mathbf{P}_{t-1}^+ \phi_{t-1}^+], \quad (17) \quad \mathbf{P}_t = \mathbf{L}_t + \mathbf{P}_{t-1}^+. \quad (18)$$

**Layer 2: Disentangled Content Representation.** This layer aims to disentangle content representation from the sequence. To model dynamic subtle content changes, the frame-wise content-aware transition model  $\mathbf{G}_t$  introduced above is applied. As shown in the orange part of Figure 1, the transition model  $\mathbf{G}_t$  is generated by a filter generator according to Equations (10), (11) and (12). Equations (13) and (14) are applied to the *predict stage* of *layer 2*.

To disentangle the content representation more effectively, in addition to equipping the layer with dynamic modeling ability, we further attempt to remove speaker information from the frame-level features for each frame during Gaussian inference. This ensures that the remaining information is more likely to be dynamic and associated with the content.

The posterior mean  $\phi^+$  and posterior precision  $\mathbf{P}^+$  of the hidden state of *layer 1* are rich with speaker information and utilized by the *update stage* of *layer 2*. Benefiting from the linear operations in this three layers design, the speaker removal operation can simply be done by subtracting the posterior mean  $\phi^+$  from features  $\mathbf{z}$  while adding the posterior covariance matrix  $(\mathbf{P}^+)^{-1}$  into the uncertainty estimation matrix  $\mathbf{L}^{-1}$ . The procedure is dynamically processed for each frame, and the *update stage* is formulated as

$$\rho_t = \Phi_t^{-1}[(\mathbf{L}_t^{-1} + (\mathbf{P}_t^+)^{-1})^{-1}(\mathbf{z}_t - \phi_t^+) + \Phi_{t-1}^+ \rho_{t-1}^+], \quad (19)$$

$$\Phi_t = (\mathbf{L}_t^{-1} + (\mathbf{P}_t^+)^{-1})^{-1} + \Phi_{t-1}^+. \quad (20)$$

**Layer 3: Disentangled Speaker Representation.** This layer uses the Gaussian inference with an identity matrix for modeling static components of the speech. Furthermore, the speaker classification loss is applied to the output of this layer and provides supervision restrictions. Different from *layer 1*, *layer 3* is designed to model the desired disentangled speaker representation by removing the content information provided by *layer 2* from the frame-level features. The procedure is similar to that in *layer 2*, and the *predict stage* is formulated as

$$\tilde{\phi}_t^+ = \tilde{\phi}_t, \quad (21) \quad \tilde{\mathbf{P}}_t^+ = \tilde{\mathbf{P}}_t, \quad (22)$$

where  $\tilde{\phi}_t^+$  and  $\tilde{\mathbf{P}}_t^+$  are the posterior mean and posterior precision, respectively. The symbol of  $\tilde{\phantom{x}}$  is used to differentiate them from the posteriors in *layer 1*. The *update stage* is formulated as

$$\tilde{\phi}_t = \tilde{\mathbf{P}}_t^{-1}[(\mathbf{L}_t^{-1} + (\Phi_t^+)^{-1})^{-1}(\mathbf{z}_t - \rho_t^+) + \tilde{\mathbf{P}}_{t-1}^+ \tilde{\phi}_{t-1}^+], \quad (23)$$

$$\tilde{\mathbf{P}}_t = (\mathbf{L}_t^{-1} + (\Phi_t^+)^{-1})^{-1} + \tilde{\mathbf{P}}_{t-1}^+. \quad (24)$$

It is worth noting that to avoid expensive matrix multiplication operations and numerically problematic matrix inversions, a simplified implementation is adopted (see Appendix A).

### 3.3 Speech Disentanglement with Self-supervision

A well-trained speaker embedding neural network requires a huge number of speakers and utterances to achieve discriminative ability. For such a large dataset, text labels are very difficult to come by. In the absence of text labels, disentangling content information from the speech is a very difficult task.

In Section 3.2, the *layer 3* of RecXi is designed to be the desired speaker representation. This is achieved by static Gaussian inference with the assumption that disentangled content representation provided by *layer 2* is reliable. We note that the disentangled speaker representation from *layer 3* is directly optimized through the classification criterion, while the optimization for disentangling content information is indirect through content removal operations in Gaussian inference. In order to ameliorate the shortcoming due to the absence of text label and to provide an extra supervisor for *layer 2*, we propose a self-supervision method to preserve speaker information via knowledge distillation in a similar fashion to those proposed in [70, 86, 9] for the teacher-student pair.

Generally speaking, large models usually outperform small models, while the small model is computationally cheaper [86]. Knowledge distillation aims to benefit a small model with the guidance of a large model. Different from the general knowledge distillation methods, our ‘teacher’ and ‘student’ are two different layers within the RecXi. Since this guidance comes from the RecXi itself, and all the training data is considered as unlabelled data for the content disentanglement task, the proposed method is considered a self-supervision method [3].

The output  $\phi$  from *layer 1* of RecXi is precursor speaker representation, and the content information remains, while *layer 2* is designed to disentangle content representation  $\rho$ . Benefiting from the linear operations used in RecXi, we can remove content information and preserve speaker representation by subtracting the content representation  $\rho$  of *layer 2* from the precursor speaker representation  $\phi$  of *layer 1*. This speaker representation is marked as  $\tilde{\phi}_{\text{lin}}$  and derived as

$$\tilde{\phi}_{\text{lin}} = \phi - \rho \quad (25)$$

where the ‘lin’ indicates that it is obtained by a **linear** operation, differing from  $\tilde{\phi}$  in *layer 3* which is disentangled by Gaussian inference. For the same input sequence, the speaker representation  $\tilde{\phi}_{\text{lin}}$  derived by this linear operation should be consistent with  $\tilde{\phi}$  obtained from disentanglement. Therefore, by restricting their difference, the gradient from supervision speaker classification loss will form a guide for *layer 2* through the linear operation in Equation (25). This serves as an extra supervisory signal different from the constraints imposed by speaker removal operation during the Gaussian inference. As  $\tilde{\phi}$  is optimized by classification loss directly, it is considered as a ‘teacher’,

while  $\tilde{\phi}_{\text{lin}}$  is a ‘student’. Since  $\tilde{\phi}_{\text{lin}}$  is derived by preserving speaker representation in Equation (25), we name the loss as **self-supervision speaker preserving loss**  $\mathcal{L}_{\text{ssp}}$ .

The  $\mathcal{L}_{\text{ssp}}$  loss can be generated by different knowledge distillation methods, a simple comparison is available in Appendix D. In this work, the idea of similarity-preserving loss [86] is in line with our layer-wise design and is inherited to guide the student towards the activation correlations induced in the teacher, instead of mimicking the teacher’s representation space directly. It is derived as

$$\mathcal{L}_{\text{ssp}} = \frac{1}{b^2} \sum_{(s,s') \in \kappa} \left\| \left( \left\| \tilde{\phi}^{(s)} \tilde{\phi}^{(s)\text{T}} \right\|_2 - \left\| \tilde{\phi}_{\text{lin}}^{(s')} \tilde{\phi}_{\text{lin}}^{(s')\text{T}} \right\|_2 \right) \right\|_F^2, \quad (26)$$

where  $\kappa$  collects all the  $(s, s')$  pairs from the same mini-batch.  $\|\cdot\|_2$  and  $\|\cdot\|_F$  indicate the row-wise L2 normalization and Frobenius norm, respectively. T indicates a transpose operation and  $b$  indicates the batch size. We define the total loss for training the framework as

$$\mathcal{L}_{\text{total}} = \alpha \mathcal{L}_{\text{cls}} + \beta \mathcal{L}_{\text{ssp}}, \quad (27)$$

where  $\mathcal{L}_{\text{cls}}$  is the speaker classification loss,  $\alpha$  and  $\beta$  are hyperparameters for balancing the total loss.

## 4 Experiments Setup

### 4.1 Dataset, Training Strategy, and Evaluation Protocol

The experiments are conducted on VoxCeleb1 [61], VoxCeleb2 [14], and the Speaker in the Wild (SITW) [55] datasets. It is worth noting that the text labels are not available for these datasets. For a fair comparison, the baselines are all re-implemented and trained with the same strategy as RecXi which follows that in ECAPA-TDNN [17]. All the models are evaluated by the performance in terms of equal error rate (EER) and the minimum detection cost function (minDCF). Detailed descriptions of datasets, training strategy, and evaluation protocol are available in Appendix C.

### 4.2 Systems Description

We evaluate the systems that are combinations of different backbone models in the encoder and different aggregation layers. To verify the compatibility of the proposed RecXi, both 2D convolution (Conv2D)-based and time delay neural network (TDNN)-based backbones are adopted:

- **1) ECAPA-TDNN** [17] is a state-of-the-art speaker recognition model based on TDNNs. The layers before the temporal aggregation layer are considered the backbone network.
- **2) ResNet** [23] and **tResNet** represent the models based on 2D convolution. The modified ResNet34 [88] is adopted as a baseline. In order to model more local regions with larger frequency bandwidths at different scales, we further modify the ResNet34 in [88] by simply changing the stride strategy and name it tResNet. The details are provided in Appendix B.

The following are temporal aggregation layers. The first three are considered baselines:

- **1) Temporal Statistics Pooling** (term as TSP from here onwards) [75] is a well-known aggregation method. It is the default option for x-vector and adopted in ResNet for speaker recognition [13, 102].
- **2) Channel- and Context-dependent Statistics Pooling** (term as Chan.&Con. from here onwards) [17] is the default aggregation layer in ECAPA-TDNN, modified from the attentive statistics pooling [62] by adding channel-dependent frame attention and allowing the self-attention produced across global properties.
- **3) Xi-vector Posterior Inference** (term as Xi from here onwards) [39] inserts uncertainty estimation into speaker embeddings as introduced in Section 3.1.
- **4) RecXi ( $\tilde{\phi}$ ) and RecXi ( $\tilde{\phi}, \tilde{\phi}_{\text{lin}}$ )** are the proposed methods. The former uses only  $\tilde{\phi}$  as the input to the decoder to derive the speaker embedding, and the latter uses a concatenation of both  $\tilde{\phi}$  and  $\tilde{\phi}_{\text{lin}}$  as the input.

Table 1: Performance in EER(%) and minDCF of the state-of-the-art (SOTA) systems and proposed RecXi on VoxCeleb1 and SITW test sets. Aug. indicates whether the system is trained with data augmentations. Para. is the number of parameters in million. Systems with † are re-implemented. The systems with ‡ following the format of ‘aggregation layer + backbone model’ are baselines. # is the index number for the implemented systems.

#	System	Aug.	Para.	VoxCeleb1-O		VoxCeleb1-H		VoxCeleb1-E		SITW <i>eval</i>	
				EER	minDCF	EER	minDCF	EER	minDCF	EER	minDCF
-	ResNet34-SKDFE [46]	✗	5.98	1.44	0.168	2.76	0.278	1.59	0.179	-	-
-	H/ASP(AAM-softmax) [37]	✗	8.0	1.25	-	2.78	-	1.56	-	-	-
-	H/ASP(AP+softmax) [37]	✗	8.0	1.21	-	2.77	-	1.42	-	-	-
-	SI-Net50 [44]	✗	-	1.28	-	2.50	-	1.28	-	2.54	-
-	RSKNet-MTSP [93]	✗	13.9	<b>1.05</b>	0.159	2.52	0.237	1.30	0.152	2.27	0.228
1	ECAPA-TDNN [17]†	✗	6.19	1.377	0.137	2.674	0.235	1.451	0.153	2.542	0.208
2	ResNet34 [88]†	✗	6.63	1.489	0.155	2.500	0.224	1.423	0.158	2.378	0.208
3	TSP + <b>proposed tResNet</b> ‡	✗	6.21	1.396	0.135	2.257	0.204	1.281	0.141	2.250	0.200
4	Xi [39] + <b>proposed tResNet</b> ‡	✗	6.54	1.295	<b>0.120</b>	2.169	0.202	1.224	0.142	2.150	0.189
5	<b>RecXi</b> ( $\tilde{\phi}, \tilde{\phi}_{lin}$ ) with $\mathcal{L}_{ssp}$ + <b>tResNet</b>	✗	7.06	1.196	0.122	<b>2.097</b>	<b>0.196</b>	<b>1.197</b>	<b>0.124</b>	<b>1.832</b>	<b>0.172</b>
-	Res2Net-26w8s [102]	✓	9.3	1.45	0.147	2.72	0.272	1.47	0.169	-	-
-	H/ASP(AAM-softmax) [37]	✓	8.0	1.15	-	2.49	-	1.35	-	-	-
-	H/ASP(AP+softmax) [37]	✓	8.0	0.88	-	2.21	-	<b>1.07</b>	-	-	-
-	ECAPA-TDNN [17]	✓	6.2	1.01	0.127	2.32	0.218	1.24	0.142	-	-
-	MFA-TDNN (standard) [48]	✓	7.32	<b>0.856</b>	0.092	2.049	0.190	1.083	0.118	-	-
-	MFA-TDNN (lite) [48]	✓	5.93	0.968	0.091	2.174	0.199	1.138	0.121	-	-
-	ECAPA-TDNN(MBFA-MW) [69]	✓	-	0.87	0.115	2.31	0.222	1.22	0.135	-	-
-	UP-LS UP-PLDA [90]	✓	-	1.01	0.124	2.18	0.224	-	-	1.59	0.167
6	ECAPA-TDNN [17]†	✓	6.19	1.127	0.145	2.249	0.223	1.194	0.133	1.668	0.155
7	ResNet34 [88]†	✓	6.63	1.101	0.128	2.221	0.208	1.252	0.139	1.584	0.161
8	Xi [39] + <b>proposed tResNet</b> ‡	✓	6.54	0.936	0.115	1.942	0.186	1.110	0.125	1.394	0.145
9	<b>RecXi</b> ( $\tilde{\phi}, \tilde{\phi}_{lin}$ ) with $\mathcal{L}_{ssp}$ + <b>tResNet</b>	✓	7.06	0.984	<b>0.091</b>	<b>1.857</b>	<b>0.179</b>	1.075	<b>0.114</b>	<b>1.340</b>	<b>0.137</b>

## 5 Results and Discussions

In Table 1, Table 2 and 3, we report the performance in terms of EER and minDCF of the proposed RecXi, various baselines and SOTA systems. It is worth noting that the VoxCeleb1-O test set is much smaller and easier compared to the other three test sets, which may lead to less convincing results.

**Comparison with SOTA methods and baselines.** In Table 1, we compare the baseline systems and proposed RecXi systems with SOTA methods. The baseline systems with proposed the tResNet backbone (system #3 and #4) achieve the SOTA performance. Compared to the TSP method (system #3), the use of Xi (system #4) achieves overall improvements with the 5.02%/4.19% average reductions in EER/minDCF. This also renders further performance improvements more difficult. By comparing systems #4 and #5, we observe that the proposed RecXi leads to relative improvements with 6.96%/5.82% average reductions in EER/minDCF compared to the Xi baseline system. The proposed RecXi (system #5) obviously further improves the performance.

**Experiments with data augmentation.** In the second half of Table 1, we report the results with augmented data (see Appendix C.2). The re-implemented ECAPA-TDNN (system #6) achieves slightly better performance than that reported in [17]. Consistent with the conclusions of training without data augmentation discussed above, the baseline (system #8) with proposed tResNet outperforms all SOTA methods and the proposed RecXi (system #9) shows great superiority over all other systems.

**Comparison for ECAPA-TDNN backbone-based systems.** The experiments discussed above are for Conv2D-based networks. For speech-related tasks, the TDNN-based networks are widely used as well [83, 17, 48, 60]. In order to verify the superiority of the proposed method under different conditions, the experiment results for the systems based on the popular ECAPA-TDNN [17] backbone

Table 2: Performance in EER(%) and minDCF of the baselines and proposed RecXi with **ECAPA-TDNN backbone** [17] on VoxCeleb1 and SITW test sets. # is the index number for the system.

#	Aggregation Layer	Params (Million)	VoxCeleb1-O		VoxCeleb1-H		VoxCeleb1-E		SITW <i>eval</i>	
			EER	minDCF	EER	minDCF	EER	minDCF	EER	minDCF
1	Chan.&Con.	6.19	1.377	0.137	2.674	0.235	1.451	0.153	2.542	0.208
10	Xi	5.90	1.340	0.140	2.647	0.237	1.429	0.148	2.679	0.204
11	<b>RecXi(<math>\tilde{\phi}</math>, <math>\tilde{\phi}_{lin}</math>) with <math>\mathcal{L}_{ssp}</math></b>	6.43	<b>1.196</b>	<b>0.107</b>	<b>2.467</b>	<b>0.227</b>	<b>1.292</b>	<b>0.141</b>	<b>2.105</b>	<b>0.184</b>

are reported in Table 2. Compared to the original aggregation layer of ECAPA-TDNN (system #1), the use of xi-vector posterior inference (system #10) performs slightly better. The comparison between system #10 and #11 presents that for the ECAPA-TDNN backbone, the proposed RecXi achieves average EER/minDCF reductions of 12.15%/10.66% over the Xi baseline.

**Brief summary.** Since the Xi baseline performs the best among all baselines and SOTA systems discussed above with different training conditions and backbone networks, we refer to it as a SOTA baseline for the following discussion. We observe that compared to the SOTA baseline, the proposed RecXi consistently improves the performance for both backbone networks on all four test sets with overall average EER/minDCF reductions of 9.56%/8.24% (system #4 vs. #5 and #10 vs. #11). The experiment results remain consistent regardless of the backbone types and whether augmented data is used. This may be due to the fact that the proposed disentanglement framework disentangles the static speaker components effectively and benefits speaker recognition. As the speaker is disentangled under the assistance of disentangled content representation, the significant improvement also proves the quality of the dynamic counterpart modeling. In addition, we found that the performance of tResNet-based systems is generally better than that of the systems with ECAPA-TDNN backbone.

Table 3: Performance in EER(%) and minDCF of various RecXi systems on VoxCeleb1 and SITW test sets for ablation study. # is the index number for the system. BN and Para. indicate the type of backbone network and number of parameters in million, respectively.

#	BN	Aggregation Layer	$\mathcal{L}_{ssp}$	Para.	VoxCeleb1-H		VoxCeleb1-E		SITW <i>eval</i>		Relative Reduction	
					EER	minDCF	EER	minDCF	EER	minDCF	EER	minDCF
11	ECAPA	RecXi( $\tilde{\phi}$ , $\tilde{\phi}_{lin}$ )	✓	6.43	2.467	<b>0.227</b>	1.292	0.141	<b>2.105</b>	<b>0.184</b>	-7.58%	-12.18%
12	ECAPA	RecXi( $\tilde{\phi}$ )	✓	6.13	<b>2.445</b>	0.233	<b>1.286</b>	<b>0.139</b>	2.160	0.191	-7.30%	-11.04%
13	ECAPA	RecXi( $\tilde{\phi}$ , $\tilde{\phi}_{lin}$ )	✗	6.43	2.477	0.228	1.326	0.142	2.351	0.196	-3.41%	-10.40%
14	ECAPA	RecXi( $\tilde{\phi}$ )	✗	6.13	2.498	0.229	1.325	0.146	2.597	0.273	Benchmark	
5	tResNet	RecXi( $\tilde{\phi}$ , $\tilde{\phi}_{lin}$ )	✓	7.06	<b>2.097</b>	0.196	<b>1.197</b>	<b>0.124</b>	1.832	<b>0.172</b>	-5.78%	-5.83%
15	tResNet	RecXi( $\tilde{\phi}$ )	✓	6.73	2.117	<b>0.192</b>	1.215	0.128	<b>1.750</b>	0.177	-6.35%	-4.82%
16	tResNet	RecXi( $\tilde{\phi}$ , $\tilde{\phi}_{lin}$ )	✗	7.06	2.130	0.198	1.222	0.128	1.886	0.184	-3.71%	-2.38%
17	tResNet	RecXi( $\tilde{\phi}$ )	✗	6.73	2.185	0.204	1.230	0.128	2.050	0.193	Benchmark	

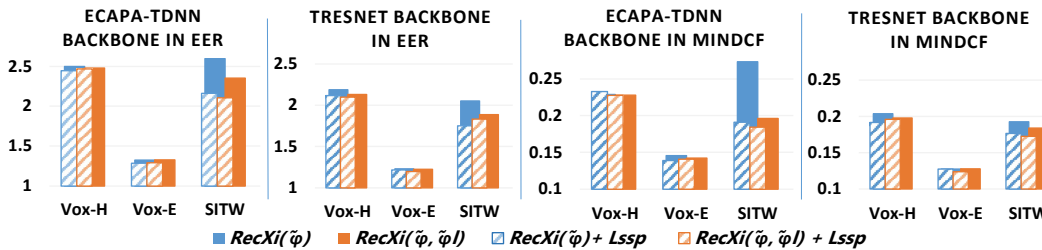


Figure 2: Bar charts for ablation studies. Performance in EER(%) and minDCF of proposed RecXi under different conditions are drawn. The blue and orange each indicate RecXi( $\tilde{\phi}$ ) and RecXi( $\tilde{\phi}$ ,  $\tilde{\phi}_{lin}$ ). Patterned color bars at the left front and solid color bars at the right behind represent the performance with and without  $\mathcal{L}_{ssp}$  for the same test trial, respectively. For all bars, the shorter the better.

**Ablation Study.** We perform ablation studies on the proposed RecXi. As the results shown in Table 3 are detailed but not intuitive, we show Figure 2 for a better view. From the charts, the following conclusions are summarized and are consistent for both ECAPA-TDNN and tResNet backbones:

1) As illustrated in Figure 2, by comparing the solid color bars with the patterned color bars while ignoring the difference of the colors, we find that most patterned color bars are shorter. It indicates that the systems with proposed self-supervision  $\mathcal{L}_{\text{ssp}}$  perform better than those without. It also proves the effectiveness of  $\mathcal{L}_{\text{ssp}}$  for RecXi frameworks. The results in Table 3 shows that the proposed self-supervision  $\mathcal{L}_{\text{ssp}}$  leads to an overall 5.07%/5.44% average reductions (system #11 vs. #13, #12 vs. #14, #5 vs. #16, #15 vs. #17) in EER/minDCF for all RecXi systems.

2) By comparing RecXi( $\tilde{\phi}$ ) shown as the solid blue color bars and RecXi( $\tilde{\phi}, \tilde{\phi}_{\text{lin}}$ ) shown as solid orange color bars, we conclude that when  $\mathcal{L}_{\text{ssp}}$  is not applied, the systems derived only from  $\tilde{\phi}$  perform worse than those using both  $\tilde{\phi}$  and  $\tilde{\phi}_{\text{lin}}$  in most of the trials (system #13 vs. #14 and #16 vs. #17). When we consider the patterned color bars, however, we find that these gaps are overcome, and very similar performance is achieved when  $\mathcal{L}_{\text{ssp}}$  is applied. We believe that the gaps between RecXi( $\tilde{\phi}$ )-based systems and RecXi( $\tilde{\phi}, \tilde{\phi}_{\text{lin}}$ )-based systems are caused by the constraints on the content disentanglement layer provided by  $\tilde{\phi}_{\text{lin}}$ . This brings RecXi( $\tilde{\phi}, \tilde{\phi}_{\text{lin}}$ ) systems an advantage in content disentanglement and further improves the efficiency of disentangling speaker representation. When both kinds of systems are enhanced by the self-supervision loss  $\mathcal{L}_{\text{ssp}}$ , a sufficient guide for disentangling content representations is provided, and it leads to a similar and improved performance. It shows the effectiveness and superiority of the proposed  $\mathcal{L}_{\text{ssp}}$  and also proves that the speaker embedding benefits from the quality of disentangled content.

Additional experiments are provided in the Appendix, covering diverse aspects including visualization, the ablation study on three RecXi layers, comparisons between RecXi and SOTA systems using ASR models or contrastive learning, as well as the evaluation of the effectiveness of  $\mathbf{G}_t$ . For details, please refer to Appendix F, G, H, and I, respectively.

## 6 Limitations

This work has some limitations: 1). The novel  $\mathcal{L}_{\text{ssp}}$  is intuitive and effective but needs further investigation and improvement. 2). As mentioned in Appendix C.2, the number of mini-transition models for deriving  $\mathbf{G}_t$  is set as  $N = 16$ . In Appendix I, we verify the effectiveness and necessity of utilizing the proposed  $\mathbf{G}_t$ . However, a comprehensive investigation of this hyperparameter is not conducted. This hyperparameter can be further exploited as it is related to the acoustic features and dynamic components we wish to disentangle.

The discussion about broader impacts is available in Appendix E.

## 7 Conclusion and Future Work

We propose the RecXi – a Gaussian inference-based disentanglement learning neural network. It models the dynamic and static components in speech signals with the aim to disentangle vocal and verbal information in the absence of text labels and benefit the speaker recognition task. In addition, a novel self-supervised speaker-preserving method is proposed to relieve the effect of text labels absent for fine content representation disentanglement. The experiments conducted on both VoxCeleb and SITW datasets prove the consistent superiority of the proposed RecXi and the effectiveness of the proposed self-supervision method. We expect that the proposed model is applicable to automatic speech recognition (ASR), where speaker-independent representation is desirable. In addition, the disentangled content and speaker embeddings are useful in the voice conversion and speech synthesis tasks. For future work, we plan to reconstruct speech signals and utilize the interaction between these two tasks to benefit each other.

## 8 Acknowledgements

This work is supported by the Agency for Science, Technology and Research (A\*STAR), Singapore, through its Council Research Fund (Project No. CR-2021-005). Haizhou Li is in part supported by the National Natural Science Foundation of China (Grant No. 62271432) and the Agency for Science, Technology and Research (A\*STAR) under its AME Programmatic Funding Scheme (Project No. A18A2b0046). The authors would like to thank the reviewers and the meta-reviewer for their comments, which greatly improved the article.

## References

- [1] Alexei Baevski, Yuhao Zhou, Abdelrahman Mohamed, and Michael Auli. wav2vec 2.0: A framework for self-supervised learning of speech representations. *Advances in Neural Information Processing Systems (NeurIPS)*, 33:12449–12460, 2020.
- [2] Zhongxin Bai and Xiao-Lei Zhang. Speaker recognition based on deep learning: An overview. *Neural Networks*, 140:65–99, 2021.
- [3] Randall Balestriero, Mark Ibrahim, Vlad Sobal, Ari Morcos, Shashank Shekhar, Tom Goldstein, Florian Bordes, Adrien Bardes, Gregoire Mialon, Yuandong Tian, et al. A cookbook of self-supervised learning. *arXiv preprint arXiv:2304.12210*, 2023.
- [4] Philipp Becker, Harit Pandya, Gregor Gebhardt, Cheng Zhao, C James Taylor, and Gerhard Neumann. Recurrent kalman networks: Factorized inference in high-dimensional deep feature spaces. In *International Conference on Machine Learning (ICML)*, pages 544–552, 2019.
- [5] Andrew Brown, Jaesung Huh, Joon Son Chung, Arsha Nagrani, and Andrew Zisserman. Voxsrc 2021: The third voxceleb speaker recognition challenge. *arXiv preprint arXiv:2201.04583*, 2022.
- [6] Danwei Cai, Weiqing Wang, and Ming Li. An iterative framework for self-supervised deep speaker representation learning. In *IEEE ICASSP*, pages 6728–6732, 2021.
- [7] Danwei Cai, Weiqing Wang, Ming Li, Rui Xia, and Chuanzeng Huang. Pretraining conformer with ASR for speaker verification. In *IEEE ICASSP*, pages 1–5, 2023.
- [8] Mathilde Caron, Ishan Misra, Julien Mairal, Priya Goyal, Piotr Bojanowski, and Armand Joulin. Unsupervised learning of visual features by contrasting cluster assignments. *Advances in Neural Information Processing Systems (NeurIPS)*, 33:9912–9924, 2020.
- [9] Keshigeyan Chandrasegaran, Ngoc-Trung Tran, Yunqing Zhao, and Ngai-Man Cheung. Re-visiting label smoothing and knowledge distillation compatibility: What was missing? In *International Conference on Machine Learning (ICML)*, pages 2890–2916, 2022.
- [10] Ting Chen, Simon Kornblith, Mohammad Norouzi, and Geoffrey Hinton. A simple framework for contrastive learning of visual representations. In *International Conference on Machine Learning (ICML)*, pages 1597–1607, 2020.
- [11] Ju chieh Chou, Cheng chieh Yeh, Hung yi Lee, and Lin shan Lee. Multi-target voice conversion without parallel data by adversarially learning disentangled audio representations. In *Proc. Interspeech*, pages 501–505, 2018.
- [12] Ju chieh Chou and Hung-Yi Lee. One-shot voice conversion by separating speaker and content representations with instance normalization. In *Proc. Interspeech*, pages 664–668, 2019.
- [13] Joon Son Chung, Jaesung Huh, Seongkyu Mun, Minjae Lee, Hee-Soo Heo, Soyeon Choe, Chiheon Ham, Sunghwan Jung, Bong-Jin Lee, and Icksang Han. In defence of metric learning for speaker recognition. In *Proc. Interspeech*, pages 2977–2981, 2020.
- [14] Joon Son Chung, Arsha Nagrani, and Andrew Zisserman. VoxCeleb2: Deep speaker recognition. In *Proc. Interspeech*, pages 1086–1090, 2018.
- [15] Rohan Kumar Das, Sarfaraz Jelil, and S. R. Mahadeva Prasanna. Significance of constraining text in limited data text-independent speaker verification. In *International Conference on Signal Processing and Communications (SPCOM)*, pages 1–5, 2016.
- [16] Jiankang Deng, Jia Guo, Niannan Xue, and Stefanos Zafeiriou. Arcface: Additive angular margin loss for deep face recognition. In *IEEE/CVF Conference on Computer Vision and Pattern Recognition (CVPR)*, pages 4690–4699, 2019.
- [17] Brecht Desplanques, Jenthe Thienpondt, and Kris Demuynck. ECAPA-TDNN: Emphasized channel attention, propagation and aggregation in TDNN based speaker verification. In *Proc. Interspeech*, pages 3830–3834, 2020.

- [18] Jacob Devlin, Ming-Wei Chang, Kenton Lee, and Kristina Toutanova. BERT: Pre-training of deep bidirectional transformers for language understanding. In *Proceedings of the Conference of the North American Chapter of the Association for Computational Linguistics: Human Language Technologies (NAACL-HLT)*, pages 4171–4186, 2019.
- [19] Subhadeep Dey, Takafumi Koshinaka, Petr Motlicek, and Srikanth Madikeri. DNN based speaker embedding using content information for text-dependent speaker verification. In *IEEE ICASSP*, pages 5344–5348, 2018.
- [20] Xiaoxue Gao, Xiaohai Tian, Yi Zhou, Rohan Kumar Das, and Haizhou Li. Personalized singing voice generation using wavernn. In *Proc. Odyssey*, pages 252–258, 2020.
- [21] Xavier Glorot, Antoine Bordes, and Yoshua Bengio. Deep sparse rectifier neural networks. In *Proceedings of the Fourteenth International Conference on Artificial Intelligence and Statistics*, pages 315–323, 2011.
- [22] Jean-Bastien Grill, Florian Strub, Florent Altché, Corentin Tallec, Pierre Richemond, Elena Buchatskaya, Carl Doersch, Bernardo Avila Pires, Zhaohan Guo, Mohammad Gheshlaghi Azar, et al. Bootstrap your own latent—a new approach to self-supervised learning. *Advances in Neural Information Processing Systems (NeurIPS)*, 33:21271–21284, 2020.
- [23] Kaiming He, Xiangyu Zhang, Shaoqing Ren, and Jian Sun. Deep residual learning for image recognition. In *IEEE/CVF Conference on Computer Vision and Pattern Recognition (CVPR)*, pages 770–778, 2016.
- [24] Georg Heigold, Ignacio Moreno, Samy Bengio, and Noam Shazeer. End-to-end text-dependent speaker verification. In *IEEE ICASSP*, pages 5115–5119, 2016.
- [25] Qian-Bei Hong, Chung-Hsien Wu, and Hsin-Min Wang. Generalization ability improvement of speaker representation and anti-interference for speaker verification. *IEEE/ACM Transactions on Audio, Speech, and Language Processing*, 31:486–499, 2023.
- [26] Wei-Ning Hsu, Benjamin Bolte, Yao-Hung Hubert Tsai, Kushal Lakhota, Ruslan Salakhutdinov, and Abdelrahman Mohamed. Hubert: Self-supervised speech representation learning by masked prediction of hidden units. *IEEE/ACM Transactions on Audio, Speech, and Language Processing*, 29:3451–3460, 2021.
- [27] Wei-Ning Hsu, Yu Zhang, and James Glass. Unsupervised learning of disentangled and interpretable representations from sequential data. In *Advances in Neural Information Processing Systems (NeurIPS)*, volume 30, pages 1878–1889, 2017.
- [28] Wei-Ning Hsu, Yu Zhang, Ron J Weiss, Yu-An Chung, Yuxuan Wang, Yonghui Wu, and James Glass. Disentangling correlated speaker and noise for speech synthesis via data augmentation and adversarial factorization. In *IEEE ICASSP*, pages 5901–5905, 2019.
- [29] Hirokazu Kameoka, Takuhiro Kaneko, Kou Tanaka, and Nobukatsu Hojo. Acvae-vc: Non-parallel voice conversion with auxiliary classifier variational autoencoder. *IEEE/ACM Transactions on Audio, Speech, and Language Processing*, 27(9):1432–1443, 2019.
- [30] P. Kenny and P. Dumouchel. Disentangling speaker and channel effects in speaker verification. In *IEEE ICASSP*, pages 37–40, 2004.
- [31] Patrick Kenny. Bayesian speaker verification with heavy-tailed priors. In *Proc. Odyssey, keynote presentation*, 2010.
- [32] Aparna Khare, Eunjung Han, Yuguang Yang, and Andreas Stolcke. ASR-aware end-to-end neural diarization. In *IEEE ICASSP*, pages 8092–8096, 2022.
- [33] Diederik P. Kingma and Jimmy Ba. Adam: A method for stochastic optimization. In *International Conference on Learning Representations (ICLR)*, 2015.
- [34] Tom Ko, Vijayaditya Peddinti, Daniel Povey, and Sanjeev Khudanpur. Audio augmentation for speech recognition. In *Proc. Interspeech*, pages 3586–3589, 2015.

- [35] Tom Ko, Vijayaditya Peddinti, Daniel Povey, Michael L. Seltzer, and Sanjeev Khudanpur. A study on data augmentation of reverberant speech for robust speech recognition. In *IEEE ICASSP*, pages 5220–5224, 2017.
- [36] Yoohwan Kwon, Soo-Whan Chung, and Hong-Goo Kang. Intra-class variation reduction of speaker representation in disentanglement framework. In *Proc. Interspeech*, pages 3231–3235, 2020.
- [37] Yoohwan Kwon, Hee-Soo Heo, Bong-Jin Lee, and Joon Son Chung. The ins and outs of speaker recognition: lessons from voxsrc 2020. In *IEEE ICASSP*, pages 5809–5813, 2021.
- [38] Anthony Larcher, Kong Aik Lee, Bin Ma, and Haizhou Li. Text-dependent speaker verification: Classifiers, databases and rsr2015. *Speech Communication*, 60:56–77, 2014.
- [39] Kong Aik Lee, Qionqiong Wang, and Takafumi Koshinaka. Xi-vector embedding for speaker recognition. *IEEE Signal Processing Letters*, 28:1385–1389, 2021.
- [40] Sang-Hoon Lee, Seung-Bin Kim, Ji-Hyun Lee, Eunwoo Song, Min-Jae Hwang, and Seong-Whan Lee. Hierspeech: Bridging the gap between text and speech by hierarchical variational inference using self-supervised representations for speech synthesis. In *Advances in Neural Information Processing Systems (NeurIPS)*, pages 16624–16636, 2022.
- [41] Yun Lei, Nicolas Scheffer, Luciana Ferrer, and Mitchell McLaren. A novel scheme for speaker recognition using a phonetically-aware deep neural network. In *IEEE ICASSP*, pages 1695–1699, 2014.
- [42] Haoqi Li, Ming Tu, Jing Huang, Shrikanth Narayanan, and Panayiotis Georgiou. Speaker-invariant affective representation learning via adversarial training. In *IEEE ICASSP*, pages 7144–7148, 2020.
- [43] Na Li, Deyi Tuo, Dan Su, Zhifeng Li, and Dong Yu. Deep discriminative embeddings for duration robust speaker verification. In *Proc. Interspeech*, pages 2262–2266, 2018.
- [44] Zhuo Li, Ce Fang, Runqiu Xiao, Wenchao Wang, and Yonghong Yan. Si-net: Multi-scale context-aware convolutional block for speaker verification. In *Proc. IEEE Automatic Speech Recognition and Understanding Workshop (ASRU)*, pages 220–227, 2021.
- [45] Jiachen Lian, Chunlei Zhang, and Dong Yu. Robust disentangled variational speech representation learning for zero-shot voice conversion. In *IEEE ICASSP*, pages 6572–6576, 2022.
- [46] Bei Liu, Haoyu Wang, Zhengyang Chen, Shuai Wang, and Yanmin Qian. Self-knowledge distillation via feature enhancement for speaker verification. In *IEEE ICASSP*, pages 7542–7546, 2022.
- [47] Lixing Liu, Sayan Ghosh, and Stefan Scherer. Towards learning nuisance-free representations of speech. In *IEEE ICASSP*, pages 6817–6821, 2018.
- [48] Tianchi Liu, Rohan Kumar Das, Kong Aik Lee, and Haizhou Li. MFA: TDNN with multi-scale frequency-channel attention for text-independent speaker verification with short utterances. In *IEEE ICASSP*, pages 7517–7521, 2022.
- [49] Tianchi Liu, Rohan Kumar Das, Kong Aik Lee, and Haizhou Li. Neural acoustic-phonetic approach for speaker verification with phonetic attention mask. *IEEE Signal Processing Letters*, 29:782–786, 2022.
- [50] Tianchi Liu, Rohan Kumar Das, Maulik Madhavi, Shengmei Shen, and Haizhou Li. Speaker-utterance dual attention for speaker and utterance verification. In *Proc. Interspeech*, pages 4293–4297, 2020.
- [51] Tianchi Liu, Maulik Madhavi, Rohan Kumar Das, and Haizhou Li. A unified framework for speaker and utterance verification. In *Proc. Interspeech 2019*, pages 4320–4324, 2019.
- [52] Yi Liu, Liang He, Jia Liu, and Michael T. Johnson. Speaker embedding extraction with phonetic information. In *Proc. Interspeech*, pages 2247–2251, 2018.

- [53] Yi Liu, Liang He, Jia Liu, and Michael T Johnson. Introducing phonetic information to speaker embedding for speaker verification. *EURASIP Journal on Audio, Speech, and Music Processing*, 19:1–17, 2019.
- [54] Yi Ma, Kong Aik Lee, Ville Hautamäki, and Haizhou Li. PL-EESR: Perceptual loss based end-to-end robust speaker representation extraction. In *Proc. IEEE Automatic Speech Recognition and Understanding Workshop (ASRU)*, pages 106–113, 2021.
- [55] Mitchell McLaren, Luciana Ferrer, Diego Castan, and Aaron Lawson. The speakers in the wild (SITW) speaker recognition database. In *Proc. Interspeech*, pages 818–822, 2016.
- [56] Zhong Meng, Jinyu Li, Zhuo Chen, Yang Zhao, Vadim Mazalov, Yifan Gong, and Biing-Hwang Juang. Speaker-invariant training via adversarial learning. In *IEEE ICASSP*, pages 5969–5973, 2018.
- [57] Zhong Meng, Yong Zhao, Jinyu Li, and Yifan Gong. Adversarial speaker verification. In *IEEE ICASSP*, pages 6216–6220, 2019.
- [58] Xiaoxiao Miao, Ian McLoughlin, Wenchao Wang, and Pengyuan Zhang. D-MONA: A dilated mixed-order non-local attention network for speaker and language recognition. *Neural Networks*, 139:201–211, 2021.
- [59] Sung Hwan Mun, Min Hyun Han, Minchan Kim, Dongjune Lee, and Nam Soo Kim. Disentangled speaker representation learning via mutual information minimization. In *Asia-Pacific Signal and Information Processing Association Annual Summit and Conference (APSIPA ASC)*, pages 89–96, 2022.
- [60] Sung Hwan Mun, Jee-weon Jung, Min Hyun Han, and Nam Soo Kim. Frequency and multi-scale selective kernel attention for speaker verification. In *IEEE Spoken Language Technology Workshop (SLT)*, pages 548–554, 2023.
- [61] Arsha Nagrani, Joon Son Chung, and Andrew Senior. VoxCeleb: A large-scale speaker identification dataset. In *Proc. Interspeech*, pages 2616–2620, 2017.
- [62] Koji Okabe, Takafumi Koshinaka, and Koichi Shinoda. Attentive statistics pooling for deep speaker embedding. In *Proc. Interspeech*, pages 2252–2256, 2018.
- [63] Zexu Pan, Ruijie Tao, Chenglin Xu, and Haizhou Li. Selective listening by synchronizing speech with lips. *IEEE/ACM Transactions on Audio, Speech, and Language Processing*, 30:1650–1664, 2022.
- [64] Alex Seungryong Park. *ASR dependent techniques for speaker recognition*. PhD thesis, Massachusetts Institute of Technology, 2002.
- [65] Daniel S Park, William Chan, Yu Zhang, Chung-Cheng Chiu, Barret Zoph, Ekin D Cubuk, and Quoc V Le. SpecAugment: A simple data augmentation method for automatic speech recognition. In *Proc. Interspeech*, pages 2613–2617, 2019.
- [66] Vijayaditya Peddinti, Daniel Povey, and Sanjeev Khudanpur. A time delay neural network architecture for efficient modeling of long temporal contexts. In *Proc. Interspeech*, pages 3214–3218, 2015.
- [67] Adam Polyak, Yossi Adi, Jade Copet, Eugene Kharonov, Kushal Lakhotia, Wei-Ning Hsu, Abdelrahman Mohamed, and Emmanuel Dupoux. Speech resynthesis from discrete disentangled self-supervised representations. In *Proc. Interspeech*, 2021.
- [68] Kaizhi Qian, Yang Zhang, Heting Gao, Junrui Ni, Cheng-I Lai, David Cox, Mark Hasegawa-Johnson, and Shiyu Chang. ContentVec: An improved self-supervised speech representation by disentangling speakers. In *International Conference on Machine Learning (ICML)*, volume 162, pages 18003–18017, 2022.
- [69] Youcai Qin, Qinghua Ren, Qirong Mao, and Jingjing Chen. Multi-branch feature aggregation based on multiple weighting for speaker verification. *Computer Speech & Language*, 77:101426, 2023.

- [70] Adriana Romero, Nicolas Ballas, Samira Ebrahimi Kahou, Antoine Chassang, Carlo Gatta, and Yoshua Bengio. Fitnets: Hints for thin deep nets. *arXiv preprint arXiv:1412.6550*, 2014.
- [71] Leda Sari, Mark Hasegawa-Johnson, and Samuel Thomas. Auxiliary networks for joint speaker adaptation and speaker change detection. *IEEE/ACM Transactions on Audio, Speech, and Language Processing*, 29:324–333, 2021.
- [72] Florian Schroff, Dmitry Kalenichenko, and James Philbin. FaceNet: A unified embedding for face recognition and clustering. In *IEEE/CVF Conference on Computer Vision and Pattern Recognition (CVPR)*, 2015.
- [73] Anna Silnova, Niko Brummer, Johan Rohdin, Themis Stafylakis, and Lukas Burget. Probabilistic embeddings for speaker diarization. In *Proc. Odyssey*, pages 24–31, 2020.
- [74] Leslie N Smith. Cyclical learning rates for training neural networks. In *IEEE winter conference on applications of computer vision (WACV)*, pages 464–472, 2017.
- [75] David Snyder, Daniel Garcia-Romero, Daniel Povey, and Sanjeev Khudanpur. Deep neural network embeddings for text-independent speaker verification. In *Proc. Interspeech*, volume 2017, pages 999–1003, 2017.
- [76] David Snyder, Daniel Garcia-Romero, Gregory Sell, Daniel Povey, and Sanjeev Khudanpur. X-vectors: Robust DNN embeddings for speaker recognition. In *IEEE ICASSP*, pages 5329–5333, 2018.
- [77] David Snyder, Pegah Ghahremani, Daniel Povey, Daniel Garcia-Romero, Yishay Carmiel, and Sanjeev Khudanpur. Deep neural network-based speaker embeddings for end-to-end speaker verification. In *IEEE Spoken Language Technology Workshop (SLT)*, pages 165–170, 2016.
- [78] Brij Mohan Lal Srivastava, Aurélien Bellet, Marc Tommasi, and Emmanuel Vincent. Privacy-preserving adversarial representation learning in ASR: Reality or illusion? In *Proc. Interspeech*, pages 3700–3704, 2019.
- [79] Guangzhi Sun, D Liu, Chao Zhang, and Philip C Woodland. Content-aware speaker embeddings for speaker diarisation. In *IEEE ICASSP*, pages 7168–7172, 2021.
- [80] Gabriel Synnaeve, Qiantong Xu, Jacob Kahn, Tatiana Likhomanenko, Edouard Grave, Vineel Pratap, Anuroop Sriram, Vitaliy Liptchinsky, and Ronan Collobert. End-to-end ASR: from supervised to semi-supervised learning with modern architectures. In *ICML 2020 Workshop on Self-supervision in Audio and Speech*, 2020.
- [81] Ruijie Tao, Kong Aik Lee, Rohan Kumar Das, Ville Hautamäki, and Haizhou Li. Self-supervised speaker recognition with loss-gated learning. In *IEEE ICASSP*, pages 6142–6146, 2022.
- [82] Ruijie Tao, Kong Aik Lee, Rohan Kumar Das, Ville Hautamäki, and Haizhou Li. Self-supervised training of speaker encoder with multi-modal diverse positive pairs. *IEEE/ACM Transactions on Audio, Speech, and Language Processing*, 31:1706–1719, 2023.
- [83] Jenthe Thienpondt, Brecht Desplanques, and Kris Demuynck. Integrating frequency translational invariance in tdnns and frequency positional information in 2d resnets to enhance speaker verification. In *Proc. Interspeech*, pages 2302–2306, 2021.
- [84] Massimiliano Todisco, Xin Wang, Ville Vestman, Md. Sahidullah, Héctor Delgado, Andreas Nautsch, Junichi Yamagishi, Nicholas Evans, Tomi H. Kinnunen, and Kong Aik Lee. ASVspoof 2019: Future horizons in spoofed and fake audio detection. In *Proc. Interspeech*, pages 1008–1012, 2019.
- [85] Katrin Tomanek, Vicky Zayats, Dirk Padfield, Kara Vaillancourt, and Fadi Biadisy. Residual adapters for parameter-efficient ASR adaptation to atypical and accented speech. In *Proceedings of the 2021 Conference on Empirical Methods in Natural Language Processing (EMNLP)*, pages 6751–6760, 2021.

- [86] Frederick Tung and Greg Mori. Similarity-preserving knowledge distillation. In *Proceedings of the IEEE/CVF International Conference on Computer Vision (ICCV)*, pages 1365–1374, 2019.
- [87] Laurens van der Maaten and Geoffrey Hinton. Visualizing data using t-sne. *Journal of Machine Learning Research*, 9:2579–2605, 2008.
- [88] Hongji Wang, Chengdong Liang, Shuai Wang, Zhengyang Chen, Binbin Zhang, Xu Xiang, Yanlei Deng, and Yanmin Qian. Wespeaker: A research and production oriented speaker embedding learning toolkit. In *IEEE ICASSP*, pages 1–5, 2023.
- [89] Qiongqiong Wang, Kong Aik Lee, and Tianchi Liu. Scoring of large-margin embeddings for speaker verification: Cosine or PLDA? In *Proc. Interspeech*, pages 600–604, 2022.
- [90] Qiongqiong Wang, Kong Aik Lee, and Tianchi Liu. Incorporating uncertainty from speaker embedding estimation to speaker verification. In *IEEE ICASSP*, pages 1–5, 2023.
- [91] Shuai Wang, Johan Rohdin, Lukáš Burget, Oldřich Plchot, Yanmin Qian, Kai Yu, and Jan Černocký. On the usage of phonetic information for text-independent speaker embedding extraction. In *Proc. Interspeech*, pages 1148–1152, 2019.
- [92] Jennifer A. Williams. *Learning disentangled speech representations*. PhD thesis, The University of Edinburgh, 2022.
- [93] Yanfeng Wu, Chenkai Guo, Junan Zhao, Xiao Jin, and Jing Xu. RSKNet-MTSP: Effective and portable deep architecture for speaker verification. *Neurocomputing*, 511:259–272, 2022.
- [94] Zhizheng Wu, Nicholas Evans, Tomi Kinnunen, Junichi Yamagishi and Federico Alegre, and Haizhou Li. Spoofing and countermeasures for speaker verification: A survey. *Speech Communication*, 66:130–153, 2015.
- [95] Weidi Xie, Arsha Nagrani, Joon Son Chung, and Andrew Zisserman. Utterance-level aggregation for speaker recognition in the wild. In *IEEE ICASSP*, pages 5791–5795, 2019.
- [96] Chang Zeng, Xin Wang, Erica Cooper, Xiaoxiao Miao, and Junichi Yamagishi. Attention back-end for automatic speaker verification with multiple enrollment utterances. In *IEEE ICASSP*, pages 6717–6721, 2022.
- [97] Haoran Zhang, Yuexian Zou, and Helin Wang. Contrastive self-supervised learning for text-independent speaker verification. In *IEEE ICASSP*, pages 6713–6717, 2021.
- [98] Jing-Xuan Zhang, Zhen-Hua Ling, and Li-Rong Dai. Non-parallel sequence-to-sequence voice conversion with disentangled linguistic and speaker representations. *IEEE/ACM Transactions on Audio, Speech, and Language Processing*, 28:540–552, 2019.
- [99] Qian Zhang, Han Lu, Hasim Sak, Anshuman Tripathi, Erik McDermott, Stephen Koo, and Shankar Kumar. Transformer transducer: A streamable speech recognition model with transformer encoders and rnn-t loss. In *IEEE ICASSP*, pages 7829–7833, 2020.
- [100] Siqi Zheng, Yun Lei, and Hongbin Suo. Phonetically-aware coupled network for short duration text-independent speaker verification. In *Proc. Interspeech*, pages 926–930, 2020.
- [101] Tianyan Zhou, Yong Zhao, Jinyu Li, Yifan Gong, and Jian Wu. CNN with phonetic attention for text-independent speaker verification. In *Proc. IEEE Automatic Speech Recognition and Understanding Workshop (ASRU)*, pages 718–725, 2019.
- [102] Tianyan Zhou, Yong Zhao, and Jian Wu. ResNeXt and Res2Net structures for speaker verification. In *IEEE Spoken Language Technology Workshop (SLT)*, pages 301–307, 2021.
- [103] Yi Zhou, Xiaohai Tian, and Haizhou Li. Language agnostic speaker embedding for cross-lingual personalized speech generation. *IEEE/ACM Transactions on Audio, Speech, and Language Processing*, 29:3427–3439, 2021.
- [104] Yi Zhou, Xiaohai Tian, Haihua Xu, Rohan Kumar Das, and Haizhou Li. Cross-lingual voice conversion with bilingual phonetic posteriorgram and average modeling. In *IEEE ICASSP*, pages 6790–6794, 2019.

## A Simplified Implementation for Gaussian Inference in RecXi

In this section, we will introduce the simplified method for implementing the proposed Gaussian inference. We take *layer 2* as an example and Equations (19) and (20) are repeated as follows:

$$\rho_t = \Phi_t^{-1}[(\mathbf{L}_t^{-1} + (\mathbf{P}_t^+)^{-1})^{-1}(\mathbf{z}_t - \phi_t^+) + \Phi_{t-1}^+ \rho_{t-1}^+], \quad (28)$$

$$\Phi_t = (\mathbf{L}_t^{-1} + (\mathbf{P}_t^+)^{-1})^{-1} + \Phi_{t-1}^+. \quad (29)$$

We formulate the adjusted uncertainty estimate  $\mathbf{L}'_t$  and point estimation with speaker representation removal  $\mathbf{z}'_t$  as following:

$$\mathbf{L}'_t = (\mathbf{L}_t^{-1} + (\mathbf{P}_t^+)^{-1})^{-1}, \quad (30)$$

$$\mathbf{z}'_t = \mathbf{z}_t - \phi_t^+. \quad (31)$$

Then, Equations (28) and (29) are simplified as

$$\rho_t = \Phi_t^{-1} \mathbf{L}'_t \mathbf{z}'_t + \Phi_t^{-1} \Phi_{t-1}^+ \rho_{t-1}^+, \quad (32)$$

$$\Phi_t = \mathbf{L}'_t + \Phi_{t-1}^+. \quad (33)$$

Similar to [39], we assume that the covariance (and precision) matrices are diagonal and choose to estimate directly the log-precision which turns out to be more convenient for following derivation. And  $\mathbf{L}'_t$  in (30) can be simplified by computing the diagonal elements directly and thereby avoiding the expensive computational for matrix inverse operations. The  $i$ -th diagonal element is formulated as

$$\mathbf{L}'_{t(i)} = \frac{\mathbf{L}_{t(i)} \mathbf{P}_{t(i)}}{\mathbf{L}_{t(i)} + \mathbf{P}_{t(i)}}. \quad (34)$$

Let gain factor  $\mathbf{A}_t = \Phi_t^{-1} \mathbf{L}'_t$  and  $\mathbf{A}_{t-1} = \Phi_t^{-1} \Phi_{t-1}^+$ , then,

$$\mathbf{A}_t = \Phi_t^{-1} \mathbf{L}'_t = [\mathbf{L}'_t + \Phi_{t-1}^+]^{-1} \mathbf{L}'_t, \quad (35)$$

$$\mathbf{A}_{t-1} = \Phi_t^{-1} \Phi_{t-1}^+ = [\mathbf{L}'_t + \Phi_{t-1}^+]^{-1} \Phi_{t-1}^+. \quad (36)$$

Therefore, the  $i$ -th diagonal element of the gain factor is computed as

$$\mathbf{A}_{t(i)} = \frac{\mathbf{L}'_{t(i)}}{\mathbf{L}'_{t(i)} + \Phi_{t-1(i)}^+} = \frac{\exp(\log(\mathbf{L}'_{t(i)}))}{\exp(\log(\mathbf{L}'_{t(i)})) + \exp(\log(\Phi_{t-1(i)}^+))}, \quad (37)$$

$$\mathbf{A}_{t-1(i)} = \frac{\Phi_{t-1(i)}^+}{\mathbf{L}'_{t(i)} + \Phi_{t-1(i)}^+} = \frac{\exp(\log(\Phi_{t-1(i)}^+))}{\exp(\log(\mathbf{L}'_{t(i)})) + \exp(\log(\Phi_{t-1(i)}^+))}. \quad (38)$$

Let  $\mathbf{K} = [\log(\mathbf{L}'_{t(i)}), \log(\Phi_{t-1(i)}^+)]$ , then  $\mathbf{A}_{t(i)}$  and  $\mathbf{A}_{t-1(i)}$  equal to the outputs of a *softmax* function ( $\sigma$ ) of  $\mathbf{K}$ .

$$\mathbf{A}_{t(i)} = \sigma(\mathbf{K})_1, \quad (39)$$

$$\mathbf{A}_{t-1(i)} = \sigma(\mathbf{K})_2. \quad (40)$$

As mentioned above, the covariance and precision matrices are estimated directly the log-precision, therefore,  $\log(\mathbf{L}'_t)$  and  $\log(\Phi_{t-1}^+)$  are estimated and used directly in (39) and (40). And Equation (32) can be simplified as

$$\rho_t = \mathbf{A}_t \mathbf{z}'_t + \mathbf{A}_{t-1} \rho_{t-1}^+. \quad (41)$$

As the gain factor  $\mathbf{A}$  is a diagonal matrix, and  $\mathbf{z}$  and  $\phi$  are vectors, the expensive matrix multiplication operations and numerically problematic matrix inversions are simplified into element-wise multiplication of diagonal elements and vectors. This is the same as the implementation of point-wise multiplication for matrices in neural networks and thus, is easy to implement based on existing toolkits.

The method above can also be applied to *layer 1* and *layer 3* of the proposed RecXi. We can simplify the implementation of the entire RecXi framework by avoiding the complex and computationally expensive matrix inverse and matrix multiplication operations.

## B Comparison between the Modified ResNet34 and Proposed tResNet34

As mentioned in Section 4.2, to model more local regions with larger frequency bandwidths at different scales, we further modify the ResNet34 backbone used in [88] by simply changing the stride strategy and naming it tResNet. The structure and outputs for both backbone models are detailed in Table 4.

Table 4: The structure and outputs comparison between modified ResNet34 in [88] and proposed tResNet34. The main difference is the stride strategy.

Layer	ResNet34		tResNet34	
	stride	Output Size	stride	Output Size
$3 \times 3, 32$	(1,1)	$32 \times F \times T$	(1,1)	$32 \times F \times T$
$\begin{matrix} 3 \times 3, 32 \\ 3 \times 3, 32 \end{matrix} \times 3$	(1,1)	$32 \times F \times T$	(2,1)	$32 \times F/2 \times T$
$\begin{matrix} 3 \times 3, 64 \\ 3 \times 3, 64 \end{matrix} \times 4$	(2,2)	$64 \times F/2 \times T/2$	(2,1)	$64 \times F/4 \times T$
$\begin{matrix} 3 \times 3, 128 \\ 3 \times 3, 128 \end{matrix} \times 6$	(2,2)	$128 \times F/4 \times T/4$	(2,2)	$128 \times F/8 \times T/2$
$\begin{matrix} 3 \times 3, 256 \\ 3 \times 3, 256 \end{matrix} \times 3$	(2,2)	$256 \times F/8 \times T/8$	(2,1)	$256 \times F/16 \times T/2$

The testing results of two backbone models are stated in Table 5. Temporal statistics pooling is applied for both backbones, which is also the default aggregation layer used in [88].

Table 5: Performance in EER(%) and minDCF of the ResNet34 in [88] and proposed tResNet34 on VoxCeleb1 and SITW test sets. # is the index number for the system.

#	Backbone	params (Million)	VoxCeleb1-O		VoxCeleb1-H		VoxCeleb1-E		SITW <i>eval</i>	
			EER	minDCF	EER	minDCF	EER	minDCF	EER	minDCF
18	ResNet34	6.63	1.489	0.155	2.500	0.224	1.423	0.158	2.378	0.208
3	tResNet34	<b>6.21</b>	<b>1.396</b>	<b>0.135</b>	<b>2.257</b>	<b>0.204</b>	<b>1.281</b>	<b>0.141</b>	<b>2.250</b>	<b>0.200</b>

The tResNet design is not claimed as one of the major contributions of this work. A thorough investigation and exploration of the tResNet mechanism will be presented in a forthcoming work.

## C Experiments Setup

### C.1 Dataset

The experiments are conducted on VoxCeleb1 [61], VoxCeleb2 [14], and the Speaker in the Wild (SITW) [55] datasets. During training, only the development partition of the VoxCeleb2 dataset is used. It contains 1,092,009 utterances from 5,994 speakers. VoxCeleb1 and SITW-eval datasets are used as the test sets. There are three test lists in the VoxCeleb1, namely VoxCeleb-O, VoxCeleb-H, and VoxCeleb-E. There is no overlapping speaker between the training and testing sets. In addition, we reserved a small portion of about 2% from the training set as the validation set. It is worth noting that the text labels are not available for these datasets. The number of speakers and utterances for these two datasets are shown in Table 6.

Table 6: Number of speakers and utterances of VoxCeleb1 and VoxCeleb2 dataset.

Data set	# Speakers	# Utterances
VoxCeleb1	1,211	148,642
VoxCeleb2	5,994	1,092,009

## C.2 Training Strategy

**Implementation** The experiments are conducted using Pytorch<sup>2</sup> and implemented in SpeechBrain<sup>3</sup>. For a fair comparison, the baselines are all re-implemented and trained with the same strategy as RecXi which follows that in ECAPA-TDNN [17]. The details are stated below:

**Configuration** The Adam [33] optimizer with cyclical learning rate scheduler [74] following triangular policy [74] is used for training all models. The maximum and minimum learning rates of the cyclical scheduler are 8e-3 and 8e-8 for ECAPA-TDNN-based systems, 3e-3 and 3e-8 for ResNet-based systems. All the samples are chunked into 3-second segments during training without augmentation. The mini-batch size is 384 for ECAPA-TDNN-based systems and 256 for ResNet-based systems considering the limitations of GPU memory. Each model is trained by two NVIDIA A5000 GPUs or NVIDIA 3090 GPUs with 24GB memory.

A total of 16 epochs are trained for each system and at the end of each epoch, the model is evaluated by the validation set to find the best checkpoint for testing. The criterion of classification loss  $\mathcal{L}_{cls}$  is additive angular margin softmax (AAM-softmax) [16] with a margin of 0.2, a scale of 30 and a weight decay of 2e-5.  $\alpha$  and  $\beta$  in Equation (27) are 1.0 and 3000, respectively, following the default setting in [86].

**Data Augmentation** For the experiments marked with data augmentation, we employ five augmentation techniques to increase the diversity of the training data. The first two follow the idea of random frame dropout in the time domain [65] and speed perturbation [34]. The remaining three are a set of reverberate data, noisy data, and a mixture of both by using RIR dataset [35]. The mini-batch size is 384 (64 original samples each with 5 augmented samples). The maximum and minimum learning rates of the cyclical scheduler are 2e-3 and 2e-8. Each model is trained by 4 or 6 NVIDIA A5000 GPUs each with 24GB memory. The other configurations are the same as the experiments without data augmentation as described above.

**Model details** The number  $N$  of mini-transition models for deriving  $\mathbf{G}_t$  is set as 16. The bottleneck feature dimension of the filter generator between two fully connected layers is set as 256. The bottleneck feature dimension of uncertainty estimation in the encoder for both xi-vector and RecXi is also 256. The channels in the convolutional frame layers of ECAPA-TDNN backbone is 512 following the default setting in [17].

For the decoder, we follow the designs in ECAPA-TDNN [17] and ResNet [88] baselines. Specifically, two fully connected (FC) layers following the aggregation layer are employed. For the ECAPA-TDNN-based systems, one batch normalization layer is applied before the first FC layer. The first FC layer produces embeddings and the other one is a classification layer. The embedding dimension is 192 for the ECAPA-TDNN-based systems and 256 for the ResNet/tResNet-based systems. The backbone network is trained together with the aggregation layer RecXi, as well as the decoder.

The code and the pre-trained models will be made available with third-party re-implementation.

## C.3 Evaluation Protocol

All the models are evaluated by the performance in terms of equal error rate (EER) and the minimum detection cost function (minDCF) with  $P_{\text{target}} = 0.01$  and  $C_{\text{FA}} = C_{\text{Miss}} = 1$ . The test trial scores are calculated by measuring the cosine similarity between embeddings. The S-norm [31] post-processing method is applied for all experiments.

## D Comparisons between Different Kinds of $\mathcal{L}_{\text{ssp}}$

In this paper, we chose the similarity-preserving (SP) loss [86] as  $\mathcal{L}_{\text{ssp}}$ , as it is more in line with our layer-wise design and the idea of speaker information preserving. The experiment results reported in Table 7 show that by using either mean squared error (MSE) loss (system #19) or SP loss (system #11) as proposed  $\mathcal{L}_{\text{ssp}}$ , there is a significant improvement compared to not using  $\mathcal{L}_{\text{ssp}}$  (system #13).

---

<sup>2</sup><https://pytorch.org/>

<sup>3</sup><https://speechbrain.github.io/>

Table 7: Performance in EER(%) and minDCF of systems without proposed  $\mathcal{L}_{\text{ssp}}$  and with different kinds of  $\mathcal{L}_{\text{ssp}}$ . The model used is ECAPA-TDNN backbone with proposed RecXi( $\tilde{\phi}$ ,  $\tilde{\phi}_{\text{lin}}$ ). # is the index number for the system.

#	Loss for Self-supervision	VoxCeleb1-O		VoxCeleb1-H		VoxCeleb1-E		SITW <i>eval</i>	
		EER	minDCF	EER	minDCF	EER	minDCF	EER	minDCF
13	Not used	1.303	0.116	2.477	0.228	1.326	0.142	2.351	0.196
19	Mean Squared Error	1.202	0.128	2.471	0.228	1.296	<b>0.136</b>	2.292	0.184
11	Similarity-Preserving	<b>1.196</b>	<b>0.107</b>	<b>2.467</b>	<b>0.227</b>	<b>1.292</b>	0.141	<b>2.105</b>	<b>0.184</b>

This proves the effectiveness of our proposed novel self-supervision method both with MSE loss and SP loss. In addition, we can observe that the system with SP loss as  $\mathcal{L}_{\text{ssp}}$  outperforms the system with MSE loss as  $\mathcal{L}_{\text{ssp}}$  in most of the trials. This shows that SP loss is more appropriate for our design.

Our novelty lies in the approach of using knowledge distillation loss to effectively guide content disentanglement without relying on textual labels, rather than finding the optimal knowledge distillation loss. However, as discussed in Section 6, it is also valuable to explore the appropriate loss function for  $\mathcal{L}_{\text{ssp}}$ . Therefore, we include Table 7 here for those who may be interested.

## E Broader Impact

This work proposes a Gaussian inference-based disentanglement learning neural network namely RecXi. It models the dynamic and static components in the speech signals with the aim to disentangle vocal and verbal information and benefit speaker recognition. The system is further enhanced by the proposed novel self-supervision  $\mathcal{L}_{\text{ssp}}$  method in the absence of text labels. The research shows great effectiveness over a variety of modern methods, and it may have a wide range of other speech-related applications, such as automatic speech recognition (ASR), voice conversion, and anonymization.

On the negative side, even though the proposed method achieves the best performance so far in the field of speaker verification, it is still not perfect and may make wrong decisions at a low possibility. Similar to existing deep learning-based solutions, the decisions made are hard to interpret. This limits its application in some critical applications, such as forensic voice comparison and banking where false acceptances are serious issues. In addition, as mentioned above and in Section 7, our next plan is to reconstruct speech signals from the disentangled representations, which can also be extended to voice conversion. The voice conversion techniques can generate audio with realistic sound, and there is an increased potential risk of harm, malicious use, and ethical issues [40]. Specifically, these systems could be misused in various manners, such as fake news generation and voice spoofing. To mitigate these issues, audio anti-spoofing (or deepfake audio detection) is studied [84, 94].

## F Visualization

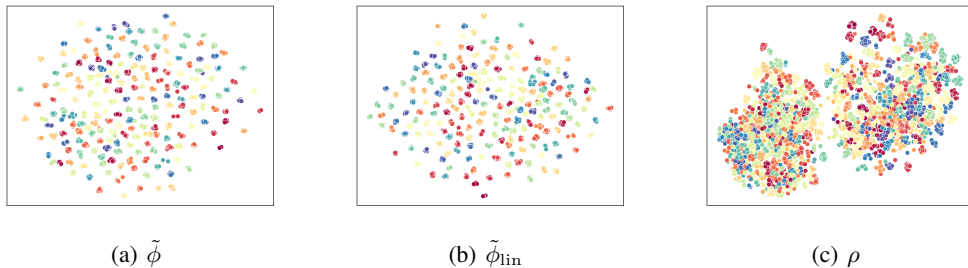


Figure 3: The t-distributed stochastic neighbor embedding (t-SNE) [87] visualization of speaker discriminative ability in embeddings space. (a) The disentangled speaker representation  $\tilde{\phi}$  from *layer* 3. (b) The speaker representation  $\tilde{\phi}_{\text{lin}}$  by the linear operation in Equation (25). (c) The content representation  $\rho$  from *layer* 2.

The visualization in Fig. 3 depicts speakers from the test set of VoxCeleb, where the first 200 speakers (indexed from id10001 to 10200) are included, each with 20 utterances. From the figure, it is evident that in *layer 3*, the disentangled speaker representation  $\tilde{\phi}$  is highly discriminative for speakers. Moreover, benefiting from the self-supervision loss, the speaker representation acquired through the linear operation in Equation (25) also exhibits notable speaker discriminative ability, comparable to that derived from *layer 3*. However, for *layer 2* ( $\rho$ ), as its main objective is to disentangle content information, it lacks the discriminative ability observed in *layer 3*.

## G Ablation Study on Three RecXi Layers

Table 8: Performance in EER(%) and minDCF of using different posteriors from the three layers of RecXi for ablation study. # is the index number for the system.

#	Posterior	Representation Description	VoxCeleb1-H		VoxCeleb1-E		SITW	
			EER	minDCF	EER	minDCF	EER	minDCF
5	$\tilde{\phi}, \tilde{\phi}_{lin}$	Disentangled Speaker & Speaker by Equation 25	<b>2.097</b>	0.196	<b>1.197</b>	<b>0.124</b>	1.832	0.172
15	$\tilde{\phi}$	Disentangled Speaker	2.117	<b>0.192</b>	1.215	0.128	<b>1.750</b>	0.177
20	$\tilde{\phi}_{lin}$	Speaker by a linear operation (Equation 25)	2.181	0.198	1.222	0.126	1.804	<b>0.172</b>
21	$\rho$	Disentangled Content	49.421	1.000	49.022	1.000	49.399	1.000
22	$\phi$	Precursor Speaker	2.187	0.199	1.249	0.131	2.023	0.186

In order to explore the information within each of RecXi’s three layers and the speaker representation achieved through a linear operation in Equation (25), we generate embeddings using the output posteriors of these layers and evaluate their speaker discriminative ability. The results in Table 8 clearly show that both  $\tilde{\phi}$  and  $\tilde{\phi}_{lin}$  (systems #5, #15, and #20) carry speaker information and demonstrate great discriminative capabilities. Additionally, reporting on *layer 2* (system #21) further supports our claims, confirming its role in representing content while effectively removing speaker-related information. The EER being close to the maximum value, 50%, indicates that *layer 2* does not contain any speaker-related information and does not exhibit any speaker discriminative ability. The precursor speaker representation  $\phi$  (system #22) also exhibits fine speaker discriminative ability, but it is slightly inferior to  $\tilde{\phi}$  (system #15). These observations align with those in Fig. 3 and strongly support our claims. Authors express their deep gratitude to anonymous reviewers for inspiring them to conduct this ablation study, which unmistakably demonstrates the success of our disentanglement approach.

## H Comparing RecXi with ASR- or Contrastive Learning-based Systems

Table 9: Performance in EER(%) and minDCF of the proposed RecXi and the SOTA systems with pre-trained ASR models [101, 7] or contrastive learning [82]. # is the index number for the system.

#	System	Params (Million)	Need Speaker Labels?	Need Pre-trained ASR Model?	VoxCeleb1-O		VoxCeleb1-H		VoxCeleb1-E	
					EER	minDCF	EER	minDCF	EER	minDCF
23	IPA [101]	>60	✓	✓	1.81	-	3.12	-	1.68	-
24	NEMO [7]	15.88	✓	✗	0.88	0.137	2.20	0.225	1.08	0.134
25	NEMO [7]	15.88	✓	✓	<b>0.74</b>	0.110	1.90	0.189	<b>0.90</b>	<b>0.105</b>
26	MCL-DPP [82]	10.5	✗	✗	2.89	-	6.27	-	3.17	-
27	MCL-DPP-C [82]	10.5	Pseudo label	✗	1.44	-	3.27	-	1.77	-
9	<b>Proposed RecXi</b>	<b>7.06</b>	✓	✗	0.984	<b>0.091</b>	<b>1.857</b>	<b>0.179</b>	1.075	0.114

As introduced in Section 1, pre-trained ASR models have been shown to be beneficial for the speaker recognition task. In this appendix section, we perform a comparison between our proposed method and the SOTA systems in two aspects: 1) using ASR models to provide phonetic information for speaker recognition [101], and 2) utilizing ASR models as initial weights [7]. It’s worth noting that [7] is a recent work that became accessible after our submission. This comparison is added during the rebuttal phase.

As shown in Table 9, our proposed system #9 not only surpasses the system employing a pre-trained ASR model (system #23) but also significantly reduces the model size. Additionally, the proposed

method achieves similar performance with the model utilizing ASR pre-training in [7] (system #9 vs #25). Our proposed method offers a significant advantage: it achieves competitive performance without requiring pre-training of an ASR model. Additionally, our method is approximately 55.5% smaller than that in [7], highlighting the efficiency and effectiveness of the proposed RecXi.

Contrastive learning has been extensively investigated and has demonstrated great performance in speaker verification. It holds the advantage of effectively utilizing unlabeled data [82]. We also compare the proposed RecXi and a SOTA contrastive learning system, both evaluated on the same dataset. Notably, even though the models in [82] incorporate extra visual information beyond speech, our proposed RecXi consistently demonstrates substantial superiority over the system detailed in [82] across all three test sets.

## I Evaluation of the Effectiveness of $\mathbf{G}_t$

Table 10: Performance in EER(%) and minDCF of using different numbers ( $N$ ) of learnable transition matrices for frame-wise content-aware transition model  $\mathbf{G}_t$  or identity matrix follows that of the xi-vector. This aims to verify the effectiveness of  $\mathbf{G}_t$ , rather than tuning the hyperparameter  $N$ . # is the index number for the system.

#	$\mathcal{L}_{\text{ssp}}$	Posterior	Number of Learnable Transition Matrices ( $N$ )	VoxCeleb1-H		VoxCeleb1-E		SITW	
				EER	minDCF	EER	minDCF	EER	minDCF
5	✓	$\tilde{\phi}, \tilde{\phi}_{\text{lin}}$	16	<b>2.097</b>	<b>0.196</b>	<b>1.197</b>	<b>0.124</b>	<b>1.832</b>	<b>0.172</b>
28	✓	$\tilde{\phi}, \tilde{\phi}_{\text{lin}}$	6	2.099	0.198	1.215	0.128	1.968	0.184
29	✓	$\tilde{\phi}, \tilde{\phi}_{\text{lin}}$	1	2.489	0.238	1.356	0.149	3.882	0.435
30	✓	$\tilde{\phi}, \tilde{\phi}_{\text{lin}}$	0 (use identity matrix)	2.524	0.260	1.471	0.165	4.280	0.435

To verify the effectiveness of  $\mathbf{G}_t$ , we conduct experiments by replacing the  $\mathbf{G}_t$  with a single learnable matrix (system #29), or an identity matrix (system #30) following that used in the xi-vector, while maintaining the three-layer design with the proposed self-supervision loss. Based on the results shown in Table 10, it is evident that using an identity matrix or a single learnable matrix leads to poor performance. This clearly demonstrates that if the second layer lacks the capacity to model dynamic patterns, the model becomes confused. This, in turn, has a significant impact on *layer 3*'s ability to obtain accurate speaker embeddings, as it relies on removing the content information provided by *layer 2*. The aforementioned observations further validate the effectiveness of the proposed  $\mathbf{G}_t$ . Furthermore, when  $N$  is set to 6 (system #28), the model achieves performance that is better than the xi-vector baseline (system #4 in Table 1) and is close to the system with  $N = 16$  (system #5) but slightly worse. This experiment demonstrates the effectiveness and necessity of our proposed  $\mathbf{G}_t$  in facilitating the capability of *layer 2* to model dynamic components.